

The Bent-End Morphology of *Treponema phagedenis* Is Associated with Short, Left-Handed, Periplasmic Flagella

NYLES W. CHARON,^{1*} STUART F. GOLDSTEIN,² KRISTINA CURCI,¹ AND RONALD J. LIMBERGER^{1,3}

Department of Microbiology and Immunology, Health Sciences Center North, West Virginia University, Morgantown, West Virginia 26506¹; Department of Genetics and Cell Biology, University of Minnesota, St. Paul, Minnesota 55108²; and Wadsworth Center for Laboratories and Research, New York State Department of Health, Albany, New York 12201-0509³

Received 20 November 1990/Accepted 15 May 1991

Treponema phagedenis Kazan 5 is a spirochete with multiple periplasmic flagella attached near each end of the cell cylinder. Dark-field microscopy revealed that most of the cell is right-handed (helix diameter, 0.23 μm ; helix pitch, 1.74 μm), and the ends appear bent. These ends could move and gyrate while the central part of the cell remained stationary. The present study examines the basis for the bent-end characteristic. Motility mutants deficient in periplasmic flagella were found to lack the bent ends, and spontaneous revertants to motility regained the periplasmic flagella and bent-end characteristic. The length of the bent ends (2.40 μm) was found to be similar to the length of the periplasmic flagella as determined by electron microscopy (2.50 μm). The helix diameter of the bent ends was 0.57 μm , and the helix pitch of the bent ends was 1.85 μm . The periplasmic flagella were short relative to the length of the cells (15 μm) and, in contrast to the reports of others, did not overlap in the center of the cell. Similar results were found with *T. phagedenis* Reiter. The results taken together indicate that there is a causal relationship between the bent-end morphology and the presence of short periplasmic flagella. We report the first three-dimensional description of spirochete periplasmic flagella. Dark-field microscopy of purified periplasmic flagella revealed that these organelles were left-handed (helix diameter, 0.36 μm ; helix pitch, 1.26 μm) and only 1 to 2 wavelengths long. Because of a right-handed cell cylinder and left-handed periplasmic flagella along with bent ends having helix diameters greater than those of either the cell cylinder or periplasmic flagella, we conclude that there is a complex interaction of the periplasmic flagella and the cell cylinder to form the bent ends. The results are discussed with respect to a possible mechanism of *T. phagedenis* motility.

Treponema phagedenis is a right-handed, helically shaped motile spirochete (25, 26, 29–31, 47, 52) with the ends reportedly left-handed (29) (moving away from an observer, a right-handed helix spirals clockwise [CW], and a left-handed helix spirals counterclockwise [CCW]). The outermost layer of the cell is a membrane sheath, and within this sheath are four to eight periplasmic flagella (PFs) attached subterminally at each end of the helical cell cylinder (25–27, 31, 52). Multiple protein species are associated with most spirochete PFs (4, 7, 9, 17, 31, 32, 39, 41, 46, 49, 53). Several lines of evidence, including immunogold (31), epitope bridging (46), and analogy to related spirochete PFs (9, 17, 53), suggest that *T. phagedenis* PFs consist of a core composed of two to four proteins of approximately 33,000 to 34,000 Da and a surface protein of approximately 39,000 Da (41). N-terminal amino acid and DNA sequence analyses indicate that the core proteins of the PFs of *T. phagedenis*, *Treponema pallidum*, and *Spirochaeta aurantia* show a high degree of homology to one another and, to a lesser extent, to flagella of other bacteria (7, 12, 40–43). 16S rRNA sequence analysis indicates that *T. phagedenis* has a close evolutionary relationship with other spirochetes. It is most akin to the main spirochete branch, which includes *T. pallidum*, *Treponema denticola*, *Spirochaeta stenostrepta*, and *Spirochaeta zuelzeri* (44, 45).

Compared with our knowledge of *Salmonella typhimurium* and *Escherichia coli* (see references 6, 34, and 35 for recent reviews), little is known about the motility of spiro-

chetes (see reference 21 for a recent review). *S. aurantia* has been proposed to swim by a mechanism whereby the PFs rotate between the sheath and the cell cylinder (2, 11, 21) in a manner analogous to flagellar rotation in rod-shaped bacteria (6, 34, 35, 51). According to this model, the rotation causes the cell cylinder to roll in one direction and the outer membrane sheath to rotate in the opposite direction (2). Both translating and nontranslating cells are observed: translating cells are believed to result from the PFs rotating in the same direction and nontranslating cells are believed to result from the PFs rotating in the opposite direction (20) (we adopt the frame of reference of viewing a swimming cell from the posterior toward the anterior end along the cell axis).

Members of the family *Leptospiraceae* swim by a mechanism that is somewhat different from that proposed for *S. aurantia* but that still assumes that the PFs rotate between the outer membrane sheath and the cell cylinder (3, 11, 13, 21, 22). In the *Leptospiraceae*, the single PF attached subterminally at each end of the cell cylinder is coiled and does not overlap in the center of the cell with the other PF (5, 10, 26). Translating cells have spiral-shaped anterior ends and hook-shaped posterior ends (3, 13, 21, 22); the ends of nontranslating cells are either both hook shaped or both spiral shaped (3, 13, 21). Motility mutants which concomitantly had an altered cell morphology and PF shape were isolated. The PFs from these mutants no longer coiled, and the ends of these mutant cells were straight (10). These results led to a model of *Leptospiraceae* motility (3), and recent evidence supports this model (13, 21, 22).

In the model of *Leptospiraceae* motility (3, 21), the shape of the cell ends is determined by the shape and direction of

* Corresponding author.

rotation of the PFs because the PF is more rigid than the cell cylinder. Rotation of the PF in one direction causes that end to be spiral shaped, and rotation in the opposite direction results in that end being hook shaped. In translating cells, the PFs at both ends are believed to rotate in the same direction as viewed from the end of the cell along the cell axis. Nontranslating cells are believed to have PFs rotating in opposite directions. In translating cells, rotation of the anterior PF causes the generation of a gyrating (i.e., bending in a circular motion without necessarily rotating, like a bent wire rotating in a rubber tube as described by Taylor [55]) spiral-shaped wave. This wave is believed to be sufficient to propel the cells forward in a pure liquid medium. The cell cylinder concomitantly rolls around the PFs in the opposite direction, which allows the cell to literally screw through a gellike medium without slippage.

Because spirochetes vary considerably in structure (23), we are extending the approach taken with the *Leptospiraceae* to gain an understanding of the motility of the structurally more complex *Treponema* spp. We have recently isolated and characterized motility mutants T-40 and T-55 of *T. phagedenis* Kazan 5, which lack PFs (31). These mutants were completely deficient in motility and lacked the multiple proteins associated with the PFs. All spontaneous revertants to motility regained the PFs and associated proteins. We report here that these PF mutants have an altered cell morphology. The results indicate that there is a causal relationship between the shape of the cell ends and the presence of short, left-handed PFs.

MATERIALS AND METHODS

Organisms and culture conditions. The origins and descriptions of wild-type *T. phagedenis* Kazan 5, motility mutants, and motility revertants have been previously reported (31). Cells were propagated in peptone-yeast extract-glucose medium supplemented with 10% rabbit serum (PYG-RS). Growth was monitored by using a Coleman model 7 photonephelometer (Coleman Instruments Inc., Oak Brook, Ill.) with readings previously correlated to cell counts (31). *T. phagedenis* Reiter, originally obtained by J. Miller from E. Hampp of the National Institute of Dental Research (54), was acquired from D. Thomas, Bowman Grey School of Medicine, Winston-Salem, N.C. *S. typhimurium* LT-2 (28) was obtained from Robert Macnab, Yale University, New Haven, Conn.

PFs and flagellar isolation. The method of isolating *T. phagedenis* PFs has previously been described (31). *S. typhimurium* flagella were isolated by the method described by Aizawa et al. (1). Sodium dodecyl sulfate-polyacrylamide gel electrophoresis and two-dimensional gel electrophoresis of purified PFs and *S. typhimurium* flagella were carried out as previously described (31, 41). The purity of these preparations was confirmed by sodium dodecyl sulfate-polyacrylamide gel electrophoresis (31, 34), two-dimensional gel electrophoresis (41), and electron microscopy (31).

Electron microscopy. All observations were made with a JEOL 100CX electron microscope. Cells were partially disrupted by using a technique similar to that reported previously (10, 31). Washed cells of *T. phagedenis* suspended in saline were treated with an equal volume of 2% deoxycholate for 1 min at 20°C. A drop was placed onto a carbon-coated Formvar copper grid (300 mesh) which had been incubated with 1% bacitracin (Sigma, St. Louis, Mo.) for 30 s. After 3 min, the fluid was drawn off and the grid was stained with 1% phosphotungstate (pH 6) for 45 s and then



FIG. 1. Diagram of a right-handed helix, showing the helix diameter and pitch (modified from reference 22).

washed with saline for 30 s. All measurements were calibrated to electron micrographs of latex beads of known diameter (Duke Scientific, Palo Alto, Calif.). Electron micrographs were enlarged 22,500 times, and PFs and cell lengths were measured with a map measurer. Computer-assisted analyses of PF length and wave form were also done. Images were digitized by tracing on a HIPAD digitizing tablet (Houston Instruments, Austin, Tex.). Each PF image was stored as a set of points 0.05 μm apart derived by linear interpolation from the entered points. Each final set of points was averaged from five tracings of the same image. To analyze PF wave form, the average value of the angles of the two line segments joining a point to the two adjacent points was taken as the tangent angle at that point. The distance between points (0.05 μm) divided by the difference between the tangent angles of two adjacent points was taken as the radius of curvature halfway between those points. Sudden increases in radius were used to locate transitions between bends for estimates of wavelengths.

Video microscopy. Cells were videotaped by placing 10 μl of cells onto a slide and then covering the cells with a 22-mm² cover glass with silicone grease along two of its edges. Cells were videorecorded by using a Leitz Ortholux microscope with a 100 \times objective, a Sony CCD camera, and a Sony VO-5800H 3/4-inch (ca. 1.9-cm) video cassette recorder. Cells were illuminated with a 200-W mercury arc lamp with a heat barrier filter. The lengths of the bent ends were determined as follows. Cells occasionally adhered spontaneously to a glass surface. The bent ends of the cells would move, and the central part of the cells would remain stationary. The bent-end length was measured from the point on the cell cylinder where the motion ceased to the tip of the cell. This region also correlated with a marked change in helix configuration. To measure the lengths of cells and bent ends, still frames were traced onto plastic transparency sheets (Write-on film; 3M, St. Paul, Minn.; 14). Cell lengths and bent-end lengths were measured with the aid of a map measurer calibrated to a video recording of a substage micrometer. Lengths are defined as distances measured along images rather than along helix axes. Photographs of still frames from the video monitor were taken with T-MAX 35-mm ASA 100 film (Kodak, Rochester, N.Y.).

Photomicroscopy. Photographs were taken and analyzed by techniques similar to those described previously (22). For photographs of live *T. phagedenis*, a cover glass supported on two sides with a mixture of Vaseline and paraffin was placed on a slide and a drop of cells in growth medium was allowed to flow under the cover glass. Cells in PYG-RS were photographed with stroboscopic illumination at a magnification of $\times 625$, with the film moving through the camera to produce single-flash exposures. For light microscopy of flagellar bundles, the stroboscope was running at 10 flashes per s and about 7 J per flash. *T. phagedenis* PFs were suspended in 0.1 M Tris-0.01 M EDTA (pH 7.8) (TE buffer), and *S. typhimurium* flagella were suspended in 0.01 M Tris-0.005 M EDTA-0.1% Triton X-100 (pH 8.0). A small drop of a suspension was placed on a slide and mixed with an

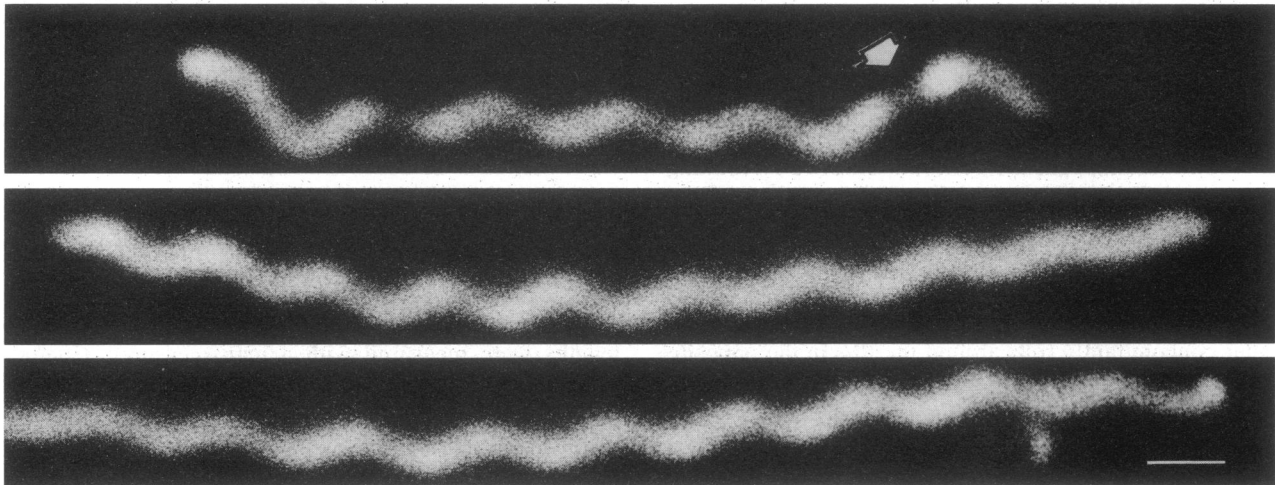


FIG. 2. Dark-field micrographs of wild-type *T. phagedenis* Kazan 5 (top), illustrating the right-handed helix in the central part of the cell and the bent ends. The plane of focus is below the axis of the cell. Arrow indicates a nonhelical bend in a bent end. The bent ends are not evident in PF-deficient mutants T-40 (middle) and T-55 (bottom). Bar, 1 μm .

approximately equal volume of 0.5% (wt/vol) solution of methylcellulose (2% = $4 \text{ N s m}^{-2} = 4,000 \text{ cP}$; MC & B, Norwood, Ohio) in TE buffer (24, 38, 50). The suspension was covered with a cover glass supported on two sides, and the bundles next to the cover glass were photographed at a magnification of $\times 800$ with the film stationary. Microscopic sectioning was carried out as described by Shimada et al. (50). The sense of winding of a helix was determined by the direction of slant of portions of the helix in photographs focused above or below the helix axis. Helix diameter and pitch are defined as previously described (22; Fig. 1). The radius of curvature was calculated from dark-field micrographs as previously described (22). Lengths of sine waves of a given amplitude and wavelength were computed by numerical integration.

RESULTS

Morphology of wild-type *T. phagedenis*. Dark-field microscopy of logarithmic-phase cells revealed that wild-type *T. phagedenis* Kazan 5 had a right-handed helix throughout most of the length of the cell (29; Fig. 2, top). There was noticeable variation of the helix diameter of the cells, with occasional cells appearing rod shaped except at the ends, which were bent. This variation in helicity was most pronounced in stationary-phase cells. Measurements of cells with the largest helical diameters yielded the following values (Table 1): helix diameter, $0.23 \pm 0.03 \mu\text{m}$ (mean \pm

standard deviation); and helix pitch, $1.74 \pm 0.12 \mu\text{m}$ ($n = 19$).

Close examination of logarithmic-phase cells indicated that *T. phagedenis* Kazan 5 had a characteristic morphology with bent ends in greater than 90% of logarithmic-phase cells (Fig. 2, top; Fig. 3). The morphology of these bent ends varied from cell to cell and even from one end of a cell to the other. These ends were consistently larger in wave form than the remainder of the cell cylinder and were generally 1 to 2 wavelengths long. The mean length of the cells was $15.42 \pm 4.86 \mu\text{m}$ ($n = 25$), and the length of the bent ends was $2.40 \pm 0.66 \mu\text{m}$ as measured along the images with a map measurer ($n = 50$; Table 1). These measurements correspond to a cell whose straight-line length, measured along the cell axis, is about $14.2 \mu\text{m}$. The helix diameter of the bent ends was $0.57 \pm 0.08 \mu\text{m}$, and the helix pitch was $1.85 \pm 0.19 \mu\text{m}$ ($n = 11$ cell ends). Video microscopy and photomicroscopy revealed that many of these bent ends were not strictly helical. Some were irregular and others were planar. Helical bent ends with these measurements would yield a length of $2.76 \mu\text{m}$, as calculated along the cell helix. Since bent ends seemed neither perfectly helical nor perfectly planar, their average length was probably between 2.40 and $2.76 \mu\text{m}$. In agreement with Kayser's results (29), those ends which were helical were left-handed. When cells were attached to a glass surface, the ends of the cells moved. Some cells adhering to a glass surface were observed with the bent ends gyrating CCW (or CW) and then reversing and gyrating CW (or

TABLE 1. Description and measurements of *T. phagedenis* Kazan 5 and isolated PFs and *S. typhimurium* flagella

Structure	Shape	Measurements (μm)		
		Helix diam	Pitch	Length
Wild type	Right-handed	0.23 ± 0.03	1.74 ± 0.12	15.42 ± 4.86
Bent ends	Variable	0.57 ± 0.08	1.85 ± 0.19	2.40 ± 0.66
Mutant T-40	Right-handed	0.26 ± 0.03	1.65 ± 0.09	ND ^a
Mutant T-55	Right-handed	0.28 ± 0.04	1.58 ± 0.15	ND
PF	Left-handed	0.36 ± 0.05	1.26 ± 0.08	2.50 ± 0.60
<i>S. typhimurium</i> flagella	Left-handed	0.47 ± 0.04	2.47 ± 0.05	

^a ND, not determined.

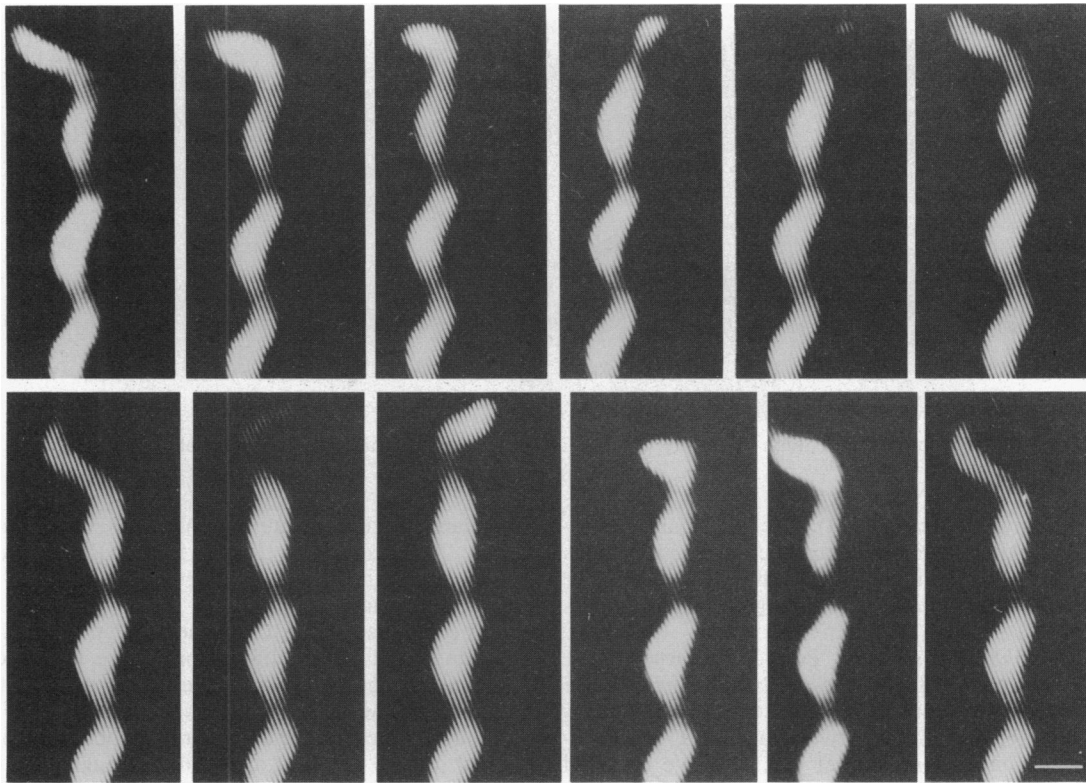


FIG. 3. Sequential photographs from a video tape of a cell tethered to a glass surface focused above the plane of the cell. The helix is right-handed; the cell helix slants from the lower left to the upper right. Top, CW gyration as viewed from the bottom of the figure (total interval = 0.3 s); bottom, CCW gyration (total interval = 0.13 s). Bar, 1 μm .

CCW), with the central part of the cell remaining stationary (Fig. 3).

Morphology of motility mutants. *T. phagedenis* Kazan 5 PF motility mutants T-40 and T-55, which fail to make PFs (31), were examined by dark-field microscopy (Fig. 2, middle and bottom). These mutants were also right-handed, with a helix pitch and diameter similar to those of the wild type. T-40 had a maximum helix diameter of $0.26 \pm 0.03 \mu\text{m}$ and a pitch of $1.65 \pm 0.09 \mu\text{m}$ ($n = 12$), while T-55 had a maximum helix diameter of $0.28 \pm 0.04 \mu\text{m}$ and a pitch of $1.58 \pm 0.15 \mu\text{m}$ ($n = 8$) (Table 1). Both mutants were considerably longer than the wild type and often grew in chains. However, mutants T-40 and T-55 were found to lack the bent-end morphology of the wild type. All six spontaneously occurring revertants to motility, which also regained the PFs (31), recovered the bent-end morphology. These results suggest that the presence of the PFs influences the shape of the cell ends.

Electron microscopy of partially disrupted cells. To understand the relationship between bent-end morphology and PF structure, the outer membrane sheaths of the cells were gently disrupted to free the PFs for visualization and characterization. Electron microscopy revealed that the PFs were considerably shorter than one-half the length of the cell cylinder, indicating that these organelles do not overlap in the center of the cell (Fig. 4). Free or broken PFs were not observed. We measured PFs which extended directly from the tip or at approximately right angles to the cell cylinder. The length of the PFs was $2.50 \pm 0.60 \mu\text{m}$ (Table 1; range, 1.17 to 3.00 μm ; $n = 50$ PFs) and was essentially identical to those of purified PFs ($2.51 \pm 0.55 \mu\text{m}$ [$n = 12$]). These

results suggest that the length of the PFs was similar to the length of the bent ends (Table 1); moreover, the wavy appearance of the PFs indicates that these filaments had a defined shape. The PFs were approximately 1 to 2 wavelengths long. The peak-to-peak amplitude of the PFs was $0.35 \pm 0.08 \mu\text{m}$ ($n = 15$), and their wavelength was $1.35 \pm 0.15 \mu\text{m}$. The length/wavelength ratio, measured along the PFs, was $1.63 \pm 0.22 \mu\text{m}$ ($n = 15$). The radii of curvature were not completely constant and tended to be somewhat larger near the ends of the bends. The average value for the five points in the middle of each of the bends was $0.42 \pm 0.12 \mu\text{m}$ ($n = 41$).

Characterization of PFs by dark-field microscopy. To characterize the helical nature of the PFs, purified PFs were examined by dark-field microscopy in the presence of methylcellulose (24, 38, 50). As a control, we compared our results with those for purified flagella from *S. typhimurium* LT-2 (Table 1). As can be seen in Fig. 5, the PFs were considerably shorter than the flagella of *S. typhimurium*. As with *S. typhimurium* flagella, the PFs were left-handed (Table 1). The PF helix diameter was $0.36 \pm 0.05 \mu\text{m}$, and the helix pitch was $1.26 \pm 0.08 \mu\text{m}$ ($n = 35$), measurements which are smaller than those of *S. typhimurium* flagella. The length/turn ratio and radius of curvature calculated from these values were 1.70 ± 0.12 and $0.41 \pm 0.05 \mu\text{m}$ ($n = 35$), respectively. These values are reasonably close to the corresponding values (amplitude, wavelength, length/wavelength ratio, and radius of curvature) as determined by electron microscopy. The flagella of *S. typhimurium* had a helix diameter of $0.47 \pm 0.04 \mu\text{m}$ and a pitch of $2.47 \pm 0.05 \mu\text{m}$ ($n = 42$), which compare reasonably well with those



FIG. 4. Electron micrograph of wild-type *T. phagedenis* Kazan 5 treated with deoxycholate. Bar, 1 μm .

values reported in the literature (34). The length and brightness of the PF bundles were quite variable. The faintest ones were about 1.5 wavelengths long, indicating that the longer and brighter ones were bundles containing variable numbers of PFs (24, 38, 50).

Analysis of *T. phagedenis* Reiter. Previous reports on the analysis of other strains of *T. phagedenis* differ from those reported here. Hovind Hougen reported that the PFs overlapped in the center of the cell in two strains of *T. phagedenis*, including *T. phagedenis* Reiter (25, 26). We checked whether the results with *T. phagedenis* Kazan 5 were directly applicable to *T. phagedenis* Reiter. We found that these two strains were morphologically similar on dark-field and electron microscopic examination. Dark-field microscopy revealed that *T. phagedenis* Reiter was right-handed and had irregular bent ends (length of bent ends, $2.22 \pm 0.67 \mu\text{m}$ [$n = 24$]; cell length, $10.44 \pm 2.16 \mu\text{m}$ [$n = 12$]). Electron microscopy indicated that the PFs were shorter ($2.86 \pm 0.36 \mu\text{m}$ [$n = 34$]) than one-half the length of the cell cylinder. These PFs were found to be left-handed by dark-field examination (not shown).

DISCUSSION

The spirochete strains used in this study have a long history. *T. phagedenis* Kazan 5 was isolated by Karimova and Kondratjev in 1940 in Russia (16), and *T. phagedenis* Reiter was isolated in the 1920s at the Kaiser-Wilhelm Institute in Berlin (15, 57). Several *Treponema* strains were isolated at the Institute in Berlin, but it is not known which of these is strain Reiter (15, 57). Although *T. phagedenis* Kazan 5 and Reiter were believed to cause syphilis (15, 16, 57), DNA hybridization experiments indicate that they are markedly different from *T. pallidum* (37, 52). Kazan strains 2, 4, 5, and 8 and strain Reiter show a high degree of DNA-DNA homology with one another (37, 52) and have

similar nutritional requirements and serological specificity (52). *T. phagedenis* Kazan 5 and Reiter have identical immunoreactivity with respect to PF antisera on Western blots (immunoblots) (32).

The microscopy results reported here for *T. phagedenis* Kazan 5 and Reiter differ from those reported by others. Hovind Hougen found that the PFs overlap in the center of the cell for two *T. phagedenis* strains (25, 26), whereas we found that the PFs are considerably shorter than one-half the length of the cells. In addition, although Cox observed by dark-field microscopy that *T. phagedenis* Kazan 8 showed helix irregularity primarily at the cell ends (19), he reported that *T. phagedenis* Reiter showed helix irregularity along the length of the cell. We find that both Kazan 5 and Reiter showed helix irregularity primarily at the cell ends.

It is difficult to understand the basis for the differences between our results and those of others. One possible explanation is that differences exist among the *T. phagedenis* stock cultures. We recently obtained two other stock cultures of *T. phagedenis* Reiter from another laboratory. Cells from one of these stocks were morphologically identical and serologically similar to the one obtained from D. Thomas; all were agglutinated by a *T. phagedenis* Kazan 5 antiserum. The cells from the other stock culture were considerably smaller, showed helix irregularity along the entire length of the cell, and failed to be agglutinated by the *T. phagedenis* Kazan 5 antiserum. Moreover, the DNA from this stock culture had a pulsed-field gel electrophoretic pattern markedly different from those of the other two Reiter stock cultures and the Kazan 5 strain (33). Because strain Reiter and the several Kazan strains share extensive immunocross-reactivity (16, 52), we suspect that this latter stock culture was mislabeled. These results suggest that the differences we observed between our results and those of others could be related to variations in stock cultures between laboratories.

The short PFs we observed by electron microscopy of

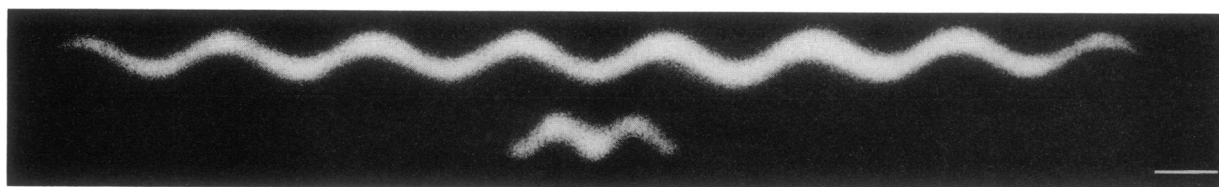


FIG. 5. Dark-field micrograph of *S. typhimurium* LT-2 flagellum (top) and *T. phagedenis* Kazan 5 PF (bottom). Bar, 1 μm .

partially disrupted cells are most likely not due to random breakage during preparation. Fragments of PFs were not observed, and the standard deviation and the range of PF length were relatively small. Both methods of determining PF length, i.e., analyzing both partially disrupted cells and purified PFs, gave essentially identical results. In addition, using the same gentle lysis treatment, we recently found that *T. denticola* yielded considerably longer PFs (greater than 5 μm) than those from *T. phagedenis*. The PFs of *T. denticola* were greater than one-half the length of the cell cylinder (48). The PFs from both species are similar with respect to multiple protein composition (18, 53) and antigenic cross-reactivity (32). These results suggest that the short PF measurements for *T. phagedenis* are not the result of problems related to methodology.

In agreement with our results, Ryter and Pillot (47) and Sykes and Miller (54) found results which suggest that the PFs of strain Reiter are less than one-half the length of the cell. Ryter and Pillot (47) believed that the PFs were stretched between the two ends of a living cell and caused the helicity of the cell body but tore into two bundles of equal length as the cell flattened on the grid during preparation for electron microscopy. By analogy with the *Leptospiraceae*, it was previously believed that each PF was attached to both ends of the cell cylinder (8), but recent evidence indicates that these PFs do not overlap (5, 10, 26). More recently, Sykes and Miller found regions of *T. phagedenis* Reiter in cross-sections in which no PFs were visible (54). These results also suggest that there are regions of the cell in which the PFs do not overlap.

Our results suggest a positive relationship between the presence of PFs, the bent-end morphology, and motility. Motility mutants which lacked the PFs failed to show the bent-end characteristic. All revertants to motility that regained the PFs recovered the bent-end morphology. In addition, the length of the bent ends as determined by dark-field microscopy (2.40 μm) approximated the length of the PFs as determined by electron microscopy (2.50 μm ; Table 1). These results taken together suggest a causal relationship between the PFs and the bent ends.

Kayser (29) reported that the bent ends are uniformly left-handed. Although we did see some ends that appeared left-handed, on many cells the bent ends appeared planar or irregular. Because there are multiple PFs at each end of the cell (25, 26, 31, 52, 53), these PFs could interact with one another and the cell cylinder in such a manner that the bent end would show a fair amount of variability. In addition, the flagella of *S. typhimurium* and *E. coli* change their helix pitch and handedness as a result of applied torque (34, 36, 50). We expect that major changes in PF shape occur as a result of different directional rotational forces applied to these organelles.

There apparently is a complex interaction of the PFs and the cell cylinder to cause the end of the cells to bend. Although the bent ends and PFs are both approximately 1 to 2 wavelengths long, the shape of the bent ends was not exactly the same as the helical forms of either the cell cylinder or the PFs. The helix of the cell cylinder is right-handed, and the PFs are left-handed (Table 1). The helix diameter of the bent ends (0.57 μm) is larger than that of both the cell cylinder (0.23 μm) and the PFs (0.36 μm). In addition, the helix pitch of the bent ends (1.85 μm) is larger than that of the PFs (1.26 μm). Thus, the bent ends are not strictly dictated by the shape of the PFs. Further analysis which defines the position of PFs within the cell will be

necessary to precisely determine how the bent ends are formed.

What do the results presented here suggest? Bacterial flagella propel the organisms by rotation (6, 34, 35, 51). We observe that the bent ends gyrate in either direction. These results suggest that, as proposed for *S. aurantia* and the *Leptospiraceae*, the PFs rotate between the sheath and the cell cylinder in *T. phagedenis*, causing the end of the cell to gyrate in either direction. *T. phagedenis* translates poorly if at all in PYG-RS medium but translates with no slippage in a gellike medium (56). In the *Leptospiraceae*, the cell rolls in one direction and the ends gyrate in the opposite direction. The torque due to the rolling of the cell cylinder is balanced by the gyration of the ends of the cell in the opposite direction (3, 13, 21, 22). As with the *Leptospiraceae*, we believe that the PFs of *T. phagedenis* are more rigid than the cell cylinder and in part dictate the shape of the cell ends. Apparently, there is insufficient thrust due to the gyration of the anterior end in *T. phagedenis* to allow for translation in low-viscosity media. Rolling of the cell cylinder, however, allows *T. phagedenis* to swim through a gellike medium. Further experiments will be necessary to determine whether the motility model (3) developed for the *Leptospiraceae* directly applies to *T. phagedenis* and other spirochetes.

ACKNOWLEDGMENTS

We thank R. Macnab and D. Thomas for strains and J. Miller for tracking down the history of his Reiter strain. We appreciate the National Institute of Occupational Safety and Health and D. Berry for use of their electron microscope. We also thank E. P. Greenberg, S. Norris, B. Paster, and C. Woese for communicating unpublished information and J. Kreiling, J. Ruby, and D. Yelton for reviewing the manuscript. We appreciate the help and encouragement of R. C. Johnson.

This research was supported by Public Health Service grant DE04645 from the National Institute of Dental Research and by Biomedical Research Support grant S07-RR05433-29 awarded to West Virginia University.

REFERENCES

1. Aizawa, S.-I., G. E. Dean, C. J. Jones, R. M. Macnab, and S. Yamaguchi. 1985. Purification and characterization of the flagellar hook-basal body complex of *Salmonella typhimurium*. *J. Bacteriol.* **161**:836-849.
2. Berg, H. C. 1976. How spirochetes may swim. *J. Theor. Biol.* **56**:269-273.
3. Berg, H. C., D. B. Bromley, and N. W. Charon. 1978. Leptospiral motility. *Symp. Soc. Gen. Microbiol.* **28**:285-294.
4. Bharier, M., and D. Allis. 1974. Purification and characterization of axial filaments of *Treponema phagedenis* biotype reiterii (the Reiter treponeme). *J. Bacteriol.* **120**:1434-1442.
5. Birch-Andersen, A., K. Hovind-Hougen, and C. Borg-Petersen. 1973. Electron microscopy of *Leptospira*. 1. *Leptospira* strain *Pomona*. *Acta. Pathol. Microbiol. Scand. Sect. B* **81**:665-676.
6. Blair, D. 1990. The bacterial flagella motor. *Semin. Cell Biol.* **1**:75-85.
7. Blanco, D. R., C. I. Champion, J. N. Miller, and M. A. Lovett. 1988. Antigenic and structural characterization of *Treponema pallidum* (Nichols strain) endoflagella. *Infect. Immun.* **56**:168-172.
8. Bradfield, J. R. G., and D. B. Carter. 1952. Electron-microscopic evidence on the structure of spirochetes. *Nature (London)* **159**:944-946.
9. Brahamsha, B., and E. P. Greenberg. 1988. A biochemical and cytological analysis of the complex periplasmic flagella from *Spirochaeta aurantia*. *J. Bacteriol.* **170**:4023-4042.
10. Bromley, D. B., and N. W. Charon. 1979. Axial filament involvement in the motility of *Leptospira interrogans*. *J. Bacteriol.* **137**:1406-1412.

11. Canale-Parola, E. 1978. Motility and chemotaxis of spirochetes. *Annu. Rev. Microbiol.* **32**:69-99.
12. Champion, C. I., J. N. Miller, M. A. Lovett, and D. R. Blanco. 1990. Cloning, sequencing, and expression of two class B endoflagellar genes of *Treponema pallidum* subsp. *pallidum* encoding the 34.5- and 31.0-kilodalton proteins. *Infect. Immun.* **58**:1697-1704.
13. Charon, N. W., G. R. Daughtry, R. S. McCuskey, and G. N. Franz. 1984. Microcinematographic analysis of tethered *Leptospira illini*. *J. Bacteriol.* **160**:1067-1073.
14. Charon, N. W., C. W. Lawrence, and S. O'Brien. 1981. Movement of antibody-coated latex beads attached to the spirochete *Leptospira interrogans*. *Proc. Natl. Acad. Sci. USA* **78**:7166-7170.
15. Christiansen, A. H. 1963. The Reiter strain of *Treponema pallidum*. *Acta. Pathol. Microbiol. Scand.* **57**:81-86.
16. Christiansen, A. H. 1964. Studies on the antigenic structure of *T. pallidum*. *Acta. Pathol. Microbiol. Scand.* **60**:123-130.
17. Cockayne, A., M. J. Bailey, and C. W. Penn. 1987. Analysis of sheath and core structures of the axial filament of *Treponema pallidum*. *J. Gen. Microbiol.* **133**:1397-1407.
18. Cockayne, A., R. Sanger, A. Ivic, R. A. Strugnell, J. H. MacDougall, R. B. Russell, and C. W. Penn. 1989. Antigenic and structural analysis of *Treponema denticola*. *J. Gen. Microbiol.* **135**:3209-3218.
19. Cox, C. D. 1972. Shape of *Treponema pallidum*. *J. Bacteriol.* **109**:943-944.
20. Fosnaugh, K., and E. P. Greenberg. 1988. Motility and chemotaxis of *Spirochaeta aurantia*: computer-assisted motion analysis. *J. Bacteriol.* **170**:1768-1774.
21. Goldstein, S. F., and N. W. Charon. 1988. Motility of the spirochete *Leptospira*. *Cell Motil. Cytoskel.* **9**:101-118.
22. Goldstein, S. F., and N. W. Charon. 1990. Multiple-exposure photographic analysis of a motile spirochete. *Proc. Natl. Acad. Sci. USA* **87**:4895-4899.
23. Holt, S. C. 1978. Anatomy and chemistry of spirochetes. *Microbiol. Rev.* **42**:114-160.
24. Hotani, H. 1976. Light microscope study of mixed helices in reconstituted *Salmonella* flagella. *J. Mol. Biol.* **106**:151-166.
25. Hovind Hougen, K. 1974. The ultrastructure of cultivable treponemes. I. *Treponema phagedenis*, *Treponema vincentii*, and *Treponema refringens*. *Acta Pathol. Microbiol. Scand. Sect. B* **82**:329-344.
26. Hovind Hougen, K. 1976. Determination by means of electron microscopy of morphological criteria of value for classification of some spirochetes, in particular treponemes. *Acta Pathol. Microbiol. Scand. Suppl.* **255**:1-41.
27. Hovind Hougen, K., and A. Birch-Andersen. 1971. Electron microscopy of endoflagella and microtubules in *Treponema Reiter*. *Acta Pathol. Microbiol. Scand. Sect. B* **79**:37-50.
28. Iino, T., and M. Enomoto. 1966. Genetic studies of non-flagellate mutants of *Salmonella*. *J. Gen. Microbiol.* **43**:315-327.
29. Kayser, A. 1979. Geometry of spirochetes. *FEMS Microbiol. Lett* **5**:95-99.
30. Kayser, A., and M. Adrian. 1978. Les spirochetes: sens de l'enroulement. *Ann. Microbiol. (Paris)* **129A**:351-360.
31. Limberger, R. J., and N. W. Charon. 1986. *Treponema phagedenis* has at least two proteins residing together on its periplasmic flagella. *J. Bacteriol.* **166**:105-112.
32. Limberger, R. J., and N. W. Charon. 1986. Antiserum to the 33,000-dalton periplasmic-flagellum protein of "*Treponema phagedenis*" reacts with other treponemes and *Spirochaeta aurantia*. *J. Bacteriol.* **168**:1030-1032.
33. Limberger, R. J., K. Curci, and N. Charon. Unpublished data.
34. Macnab, R. M. 1987. Flagella, p. 70-83, and Motility and chemotaxis, p. 732-759. In F. C. Neidhardt, J. L. Ingraham, K. B. Low, B. Magasanik, M. Schaechter, and H. E. Umbarger (ed.), *Escherichia coli* and *Salmonella typhimurium*: cellular and molecular biology, vol. I. American Society for Microbiology. Washington, D.C.
35. Macnab, R. M., and S.-I. Aizawa. 1984. Bacterial motility and the bacterial flagellar motor. *Annu. Rev. Biophys. Bioeng.* **13**:51-83.
36. Macnab, R. M., and M. K. Ornston. 1977. Normal-to-curly flagellar transitions and their role in bacterial tumbling. Stabilization of an alternative quaternary structure by mechanical force. *J. Mol. Biol.* **112**:1-30.
37. Miao, R., and A. H. Fieldsteel. 1978. Genetics of *Treponema*: relationship between *Treponema pallidum* and five cultivable treponemes. *J. Bacteriol.* **133**:101-107.
38. Miki-Noumura, T. 1990. Dark-field microscopic study of microtubules in solution. *Int. Rev. Cytol.* **122**:65-104.
39. Nauman, R. K., S. C. Holt, and C. D. Cox. 1969. Purification, ultrastructure, and composition of axial filaments from *Leptospira*. *J. Bacteriol.* **98**:264-380.
40. Norris, S. Personal communication.
41. Norris, S. J., N. W. Charon, R. G. Cook, M. D. Fuentes, and R. J. Limberger. 1988. Antigenic relatedness and N-terminal sequence homology define two classes of periplasmic flagellar proteins of *Treponema pallidum* subsp. *pallidum* and *Treponema phagedenis*. *J. Bacteriol.* **170**:4072-4082.
42. Pallesen, L., and P. Hindeross. 1989. Cloning and sequencing of a *Treponema pallidum* gene encoding a 31.3-kilodalton endoflagellar subunit (FlaB2). *Infect. Immun.* **57**:2166-2172.
43. Parales, J., Jr., and E. P. Greenberg. 1991. N-terminal amino acid sequences and amino acid compositions of the *Spirochaeta aurantia* flagellar filament polypeptides. *J. Bacteriol.* **173**:1357-1359.
44. Paster, B., and C. Woese. Personal communication.
45. Paster, B. J., E. Stackebrandt, R. B. Hespell, C. M. Hahn, and C. R. Woese. 1984. The phylogeny of the spirochetes. *Syst. Appl. Microbiol.* **5**:337-352.
46. Radolf, J. D., D. R. Blanco, J. N. Miller, and M. A. Lovett. 1986. Antigenic interrelationship between endoflagella of *Treponema phagedenis* biotype Reiter and *Treponema pallidum* (Nichols): molecular characterization of endoflagellar proteins. *Infect. Immun.* **54**:626-634.
47. Ryter, A., and J. Pillot. 1963. Etude au microscope electronique de la structure externe et interne du treponeme Reiter. *Ann. Inst. Pasteur (Paris)* **104**:496-501.
48. Ruby, J., and N. Charon. Unpublished data.
49. Sand Petersen, C., N. S. Pedersen, and N. H. Axelson. 1981. A simple method for the isolation of flagella from *Treponema Reiter*. *Acta Pathol. Microbiol. Scand. Sect. C* **89**:379-385.
50. Shimada, K., R. Kamiya, and S. Asakura. 1975. Left-handed to right-handed conversion in *Salmonella* flagella. *Nature (London)* **254**:332-334.
51. Silverman, M. R., and M. I. Simon. 1974. Flagellar rotation and the mechanism of bacterial motility. *Nature (London)* **249**:73-74.
52. Smibert, R. M. 1984. Genus III. *Treponema* Schaudinn 1905, 728^{AL}, p. 49-57. In N. R. Krieg and J. G. Holt (ed.), *Bergey's manual of systematic bacteriology*, vol. 1. The Williams & Wilkins Co., Baltimore.
53. Strugnell, R., A. Cockayne, and C. W. Penn. 1990. Molecular and antigenic analysis of treponemes. *Crit. Rev. Microbiol.* **17**:231-250.
54. Sykes, J. A., and J. M. Miller. 1973. Ultrastructural studies of treponemes. Location of axial filaments and some dimensions of *Treponema pallidum* (Nichols strain), *Treponema denticola*, and *Treponema reiteri*. *Infect. Immun.* **7**:100-110.
55. Taylor, G. 1952. The action of waving cylindrical tails in propelling microscopic organisms. *Proc. R. Soc. London A* **211**:225-239.
56. Van Weelden, G. J., N. W. Charon, and S. J. Norris. 1990. Abstr. 90th Annu. Meet. Am. Soc. Microbiol. 1990, I76, p. 211.
57. Wallace, A. L. 1967. Reiter treponeme. A review of the literature. *Bull. W.H.O.* **36**(Suppl.):1-103.